

Bonding, Metal-Atom Dynamics and Hyperfine Interactions of η -Phosphohlyl- and η -Pentaphosphohlyliron Complexes

Rolfe H. Herber,^{*[a]} Israel Nowik,^[a] Dmitry A. Loginov,^[b] Zoya A. Starikova,^[b] and Alexander R. Kudinov^[b]

Keywords: Iron / Mössbauer spectroscopy / P ligands / Sandwich compounds / Spin–lattice relaxation

A number of structurally related sandwich compounds of iron, in which the central metal atom is ligated to rings containing one or five phosphorus atoms, have been investigated by temperature-dependent ^{57}Fe Mössbauer spectroscopy, differential scanning calorimetry and single-crystal X-ray diffraction. The quadrupole hyperfine interaction at 90 K evidences a linear dependence on the number of ring phosphorus atoms, decreasing by about $0.35\text{ mm}\cdot\text{s}^{-1}$ for each ring carbon atom replaced by P. This effect is directly related to the

change in the overlap between metal atom d-orbitals and ligand 3s,3p or 2s,2p orbitals due to an increase in the respective bond lengths. Several one-electron oxidation products of these compounds, which are paramagnetic, have also been examined and show spin–lattice relaxation rates which are fast compared to the characteristic Mössbauer timescale of 98 ns at all temperatures above 90 K.

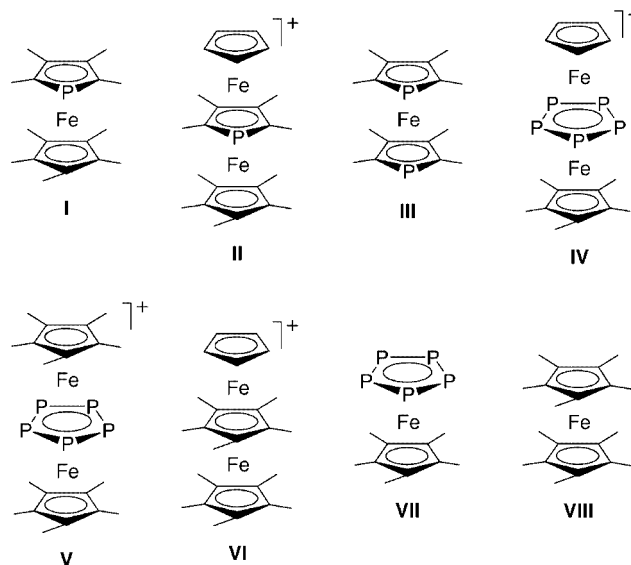
(© Wiley-VCH Verlag GmbH & Co. KGaA, 69451 Weinheim, Germany, 2004)

Introduction

In a recent detailed study, Kudinov et al.^[1] have discussed the synthesis, electrochemistry, and chemical reactivity of η -pentaphosphohlyl complexes of iron and ruthenium, including a number of double- and triple-decker sandwich compounds. In a continuation of previous research^[2] in which temperature-dependent ^{57}Fe Mössbauer spectroscopy was used, in the present study the metal-atom lattice dynamics and hyperfine interactions of the central atom in the phosphorus-containing ferrocene-like complexes of Kudinov et al.^[1] have been examined in detail over the temperature range 90 to 350 K (where appropriate). In addition, as needed, differential scanning calorimetry and magnetic susceptibility measurements have been carried out to extend these spectroscopic results. Such studies can shed light not only on the relationship between the dynamic properties of the iron atom and the details of the local molecular architecture, but also on the spin–lattice dynamics of such systems.

Among the complexes included in this study are $[\text{Cp}^*\text{Fe}(\eta\text{-C}_4\text{Me}_4\text{P})]$ (**1**) ($\text{Cp}^* = \eta\text{-C}_5\text{Me}_5$), $[\text{Cp}^*\text{Fe}(\mu\text{-}\eta\text{-}\eta\text{-C}_4\text{Me}_4\text{P})\text{FeCp}]\text{PF}_6$ (**2**) ($\text{Cp} = \eta\text{-C}_5\text{H}_5$), $[\text{Fe}(\eta\text{-C}_4\text{Me}_4\text{P})_2]$ (**3**), $[\text{Cp}^*\text{Fe}(\mu\text{-}\eta\text{-}\eta\text{-P}_5)\text{FeCp}]\text{PF}_6$ (**4**), $[\text{Cp}^*\text{Fe}(\mu\text{-}\eta\text{-}\eta\text{-P}_5)\text{FeCp}^*]\text{BF}_4$ (**5**), $[\text{Cp}^*\text{Fe}(\mu\text{-}\eta\text{-}\eta\text{-Cp}^*)\text{FeCp}]\text{PF}_6$ (**6**), $[\text{Cp}^*\text{Fe}(\eta\text{-P}_5)]$

(**7**), and $[\text{FeCp}^*_2]$ (**8**) (the anions are omitted in the chart given below).



Single crystal X-ray diffraction data for **3** have also been acquired in the present study and are reported herein.

Results and Discussion

The Mössbauer spectra of all the compounds examined in this study consist of well-resolved doublets, and a typical spectrum (of **5**) is shown in Figure 1. The hyperfine parameters at 90 K — the isomer shift (IS), the quadrupole split-

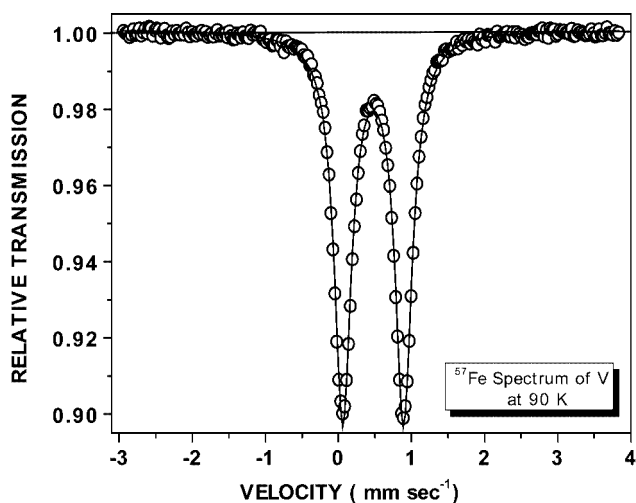
^[a] Racah Institute of Physics, The Hebrew University of Jerusalem, 91904 Jerusalem, Israel
E-mail: herber@vms.huji.ac.il

^[b] A. N. Nesmeyanov Institute of Organoelement Compounds, 28 ul. Vavilova, 119991 Moscow, GSP-1, Russian Federation
E-mail: arkudinov@ineos.ac.ru

Table 1. ^{57}Fe Mössbauer parameters of the compounds discussed in the text; the parenthetical numbers accompanying the parameters are the experimental errors in the last significant figure(s)

	1	2	3	4	5	6	7	8	Units
IS(90)	0.500(4)	0.492(5)	0.501(4)	0.469	0.477(4)	0.515(4)	0.461(3)	0.502(2)	$\text{mm}\cdot\text{s}^{-1}$
QS(90)	2.202(4)	2.248(5)	2.027(4)	0.880	0.830(4)	2.541(4)	0.639(3)	2.479(2)	$\text{mm}\cdot\text{s}^{-1}$
$-\text{dIS}/\text{dT}$	4.70(6)	3.82(15)	5.08	4.84(13)	4.85(11)	4.78(4)	6.05	5.06(9)	$\text{mm}\cdot\text{s}^{-1}\cdot\text{K}^{-1} \times 10^4$
M_{eff}	89	109	82	86	86 ± 2	86 ± 6	69 ± 2		dalton
$-\text{d} \ln A/\text{dT}$	4.64(4)	16.2(4)	7.56	12.89(4)	4.43	6.81(5)	10.6(6)	15.5(3)	$\text{K}^{-1} \times 10^3$
Θ_{M}	137	66	112	84	143	115	103	78	K

ting, (QS) — as well as the temperature dependence of the logarithm of the recoil-free fraction (f) and of the IS, and the parameters derived therefrom, are summarized in Table 1. All IS's are referred to the center of a room temperature α -Fe absorber spectrum. In several cases, as will be noted below, the spectra also revealed the presence of a small quantity of an impurity which is the unavoidable consequence of the synthetic procedures. In these cases, appropriate corrections, especially to the spectral area calculations, were applied as needed.

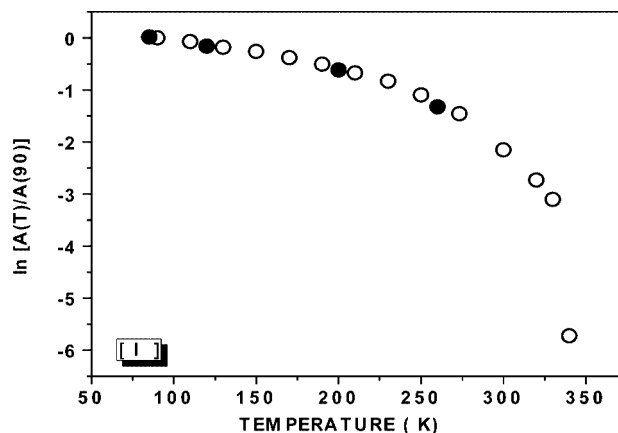
Figure 1. Mössbauer spectrum of **5** at 90 K; the velocity scale is with respect to the centroid of a room temperature α -Fe absorber spectrum

Compound 1

As will be noted from Table 1, the IS at 90 K is very similar to that of decamethylferrocene (**8**),^[3] but somewhat smaller than that of the parent ferrocene itself ($0.537 \text{ mm}\cdot\text{s}^{-1}$), in agreement with the earlier conclusion^[4] that ring substitution of H by CH_3 influences the s-electron density at the iron atom in only a very minor way. In contrast, the difference in the QS is smaller in **1** than in **8** by $0.277 \text{ mm}\cdot\text{s}^{-1}$, indicating a significant change in the details of the metal-ligand overlap when one of the ring CH groups is replaced by a phosphorus atom, an observation which will be further developed below. The temperature dependence of the IS in the high temperature limit (190–330 K) is well fitted by a linear regression, $[(4.70 \pm 0.06) \times 10^{-4}$

$\text{mm}\cdot\text{s}^{-1}\cdot\text{K}^{-1}]$ with a correlation coefficient (R) of 0.998 for 10 data points. The effective vibrating mass, M_{eff} , calculated from these data is 88 ± 2 daltons. The difference between this value and the “bare” iron atom value of 57 daltons is, of course, a reflection of the covalency of the metal–ring interaction, and is similar to the values reported for other ferrocene-related solids. Rayon and Frenking^[5] have estimated the bonding interaction in ferrocene to be 45% coulombic and 55% covalent, and it is reasonable to assume that a comparable partitioning occurs in the present case.

The temperature dependence of the logarithm of the recoil-free fraction, $f = e^{-k^2x^2}$, which is given by the temperature dependence of the logarithm of the area, A , under the resonance curve for an optically “thin” absorber of **1**, is summarized graphically in Figure 2.

Figure 2. Temperature dependence of $\ln A$ for **1**; the open circles represent data acquired in a warming mode from 90 K, the full circles data acquired in a cooling mode following the measurement at 340 K

It is seen that although the data are completely reversible (filled versus open data points), the results are not at all well fitted by a linear regression, and, in fact, f becomes vanishingly small at temperatures above about 340 K. It should be noted that this temperature is significantly smaller than the melting point of the neat solid. These results have been associated^[2,6] with the onset of ring rotation which, in the case of two five-membered rings, one of which has five methyl substituents and the other one (or more) ring substituents of very different steric requirements, such as an H or a ring P atom, leads to a librational motion of

the two rings relative to each other. This librational motion, in turn, results in the presence of low-frequency optical modes which can take up the recoil of the gamma absorption, and hence significantly reduce the f value of the iron atom, as has been observed in a number of octamethyl ferrocene complexes.

Finally, it is worth noting that the resonance spectra of **1** do not show any significant motional anisotropy of the iron atom of the kind noted^[7] in other ferrocene-related solids, over the entire temperature range noted above.

Compound 2

As before, the hyperfine parameters at 90 K are included in Table 1. The IS is, as expected, very similar to that observed in **1** and in this context it is clear that the presence of an additional FeCp entity does not change this parameter (or the QS) significantly. However, it is worth noting that while the presence of two different Fe atoms in the structure cannot be resolved from the hyperfine parameters, the line widths in such compounds are invariably significantly larger than in compounds with only one kind of metal atom in the structure. In the case of **1** and **2** at the same temperature, this difference corresponds to a line width increase of about $0.050 \text{ mm}\cdot\text{s}^{-1}$. A fit of the data for **2** with two equally intense doublets of natural line width yields a somewhat better χ^2 than that with one doublet of broad lines. The difference in QS between the two doublets is about $0.17 \text{ mm}\cdot\text{s}^{-1}$. The QS is similar to that observed in **1** as a necessary consequence that both iron atoms “see” a single phospholyl ring in one direction, and a hydrocarbon ring in the opposite direction.

The temperature-dependence of $\ln f$ is linear above 170 K, and in this case does not show the sharp decrease observed in **1**, although this may be due to the fact that the maximum temperature used in this case was below the point where ring librational motion becomes significant. On the other hand, the temperature dependence of the area ratio in **2** evidences a significant motional anisotropy, as summarized graphically in Figure 3. It should also be noted that the temperature dependence of $\ln f$ is exceptionally large, leading to a rather “soft” covalent lattice as “seen” by the metal atom in this structure.

Compound 3

The Mössbauer parameters of this complex (Table 1) show, as expected, almost the same IS, but again a twofold decrease in the QS relative to compound **1**. The temperature dependence of the IS is linear over almost the entire range, except at the higher limit, for reasons that will be discussed below. The temperature dependence of the QS as well is nearly negligible over the entire range except at the highest temperatures. What is most remarkable about **3** is the temperature-dependence of $\ln f$, which is summarized graphically in Figure 4. It will be immediately apparent that $\ln f$ is only moderately temperature dependent to about 338 K, and then drops sharply, becoming experimentally unobservable at temperatures above 340 K. It should be noted that

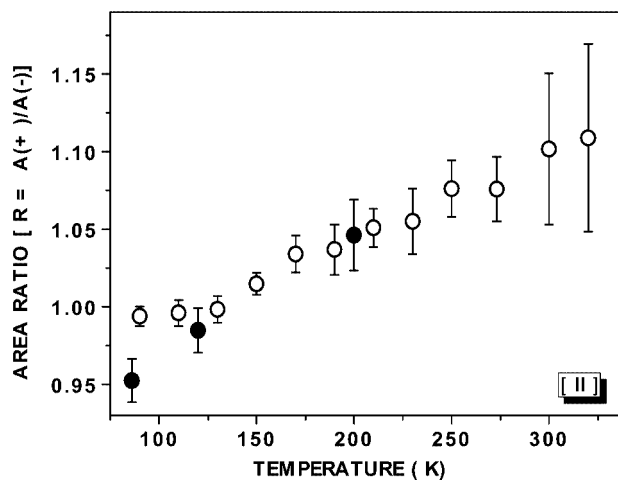


Figure 3. The temperature dependence of the area ratio for **2**; the non-unity value in the low temperature limit is presumed to arise from the temperature-independent texture effect of preferential crystallite orientation in the sample holder

the melting point of this compound is about 464 K, and has not been reported earlier in the literature.^[8] Again, this f anomaly, which occurs some 123°C below the melting point, is associated with the onset of librational motion of the two rings relative to each other. Strong supporting evidence for this interpretation is provided by the differential scanning calorimetry data summarized in Figure 5. The DSC data show a very sharp endothermic peak, starting at about 339 K and reaching a maximum at 341.8 K. On cooling, the exotherm is similarly sharp, with a maximum at 329 K. The 12.8 K hysteresis is also evident in the $\ln f$ data summarized in Figure 4, in which the cooling data, represented by the filled circles, do not evidence an experimentally observable resonance effect until a temperature of about 310 K is reached in this regime.

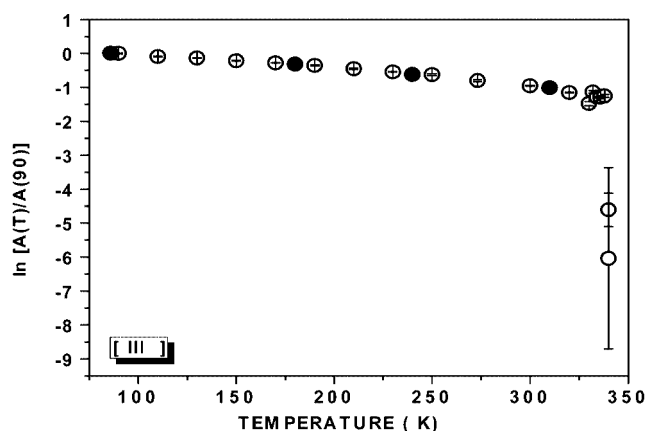


Figure 4. Temperature-dependence of $\ln A$ for **3**; the open circles pertain to data acquired in a warming mode, while the full circles represent data acquired in a cooling mode after the highest temperature point had been obtained

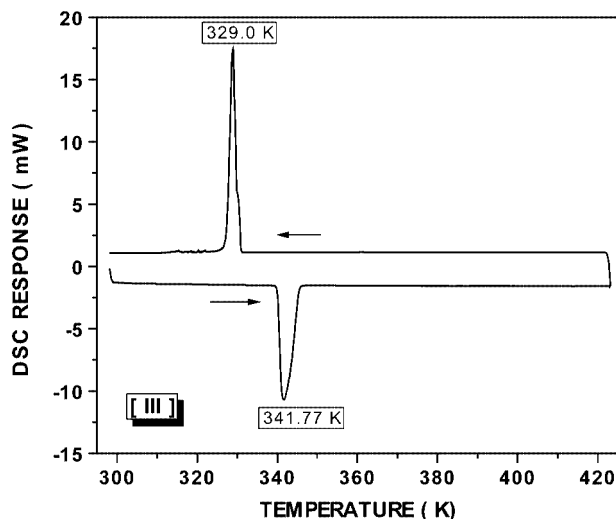


Figure 5. Differential scanning calorimetry data for **3** showing both the warming and cooling data; the approximate 12 degree hysteresis is also evident in the Mössbauer data, as discussed in the text

Compound 4

This compound is closely related to the pentaphospholyliron complex **7** described earlier,^[9,10] with two significant differences: there is an additional FeCp group attached to the phosphorus ring, and the whole complex carries a positive charge, which is balanced by a PF_6^- counterion. The hyperfine interactions at 90 K and the derived parameters are included in Table 1. As noted above, despite the differences in the ligands attached to the two iron atoms, the Mössbauer parameters of the two metal atoms are sufficiently similar that they cannot be distinguished from each other. The IS (90 K) values of **4** and **7** are essentially identical, while the QS (90 K) values differ by about $0.24 \text{ mm}\cdot\text{s}^{-1}$. It should be kept in mind, however, that the QS value for **4** reflects an average of the two different metal centers. Moreover, this parameter is nearly temperature independent in the range 90–300 K, and on further warming shows a pronounced negative slope to 350 K, while the temperature dependence of $\ln f$ is well fitted by a linear regression $[-(11.52 \pm 0.07) \times 10^{-3} \text{ K}^{-1}$; correlation coefficient: 0.993 for 21 data points] over the temperature range 90–350 K, and shows no discontinuity at about 300 K.

The spectra of **4** show two well-resolved maxima over the entire temperature range rather than the broadened collapsed spectrum characteristic of one-electron oxidized ferrocenoids, as reported earlier.^[6,11] To substantiate the expected paramagnetic nature of **4**, the magnetic susceptibility of the compound (as well as of **6**) was determined over the temperature range 6–100 K under a field of 39 Oe; the results are summarized in Figure 6.

The experimental data were fitted by using the Curie–Weiss law $\chi = \chi_0 + C/(T - \theta)$, where χ_0 is the temperature-independent susceptibility, C is the Curie constant and θ is the Curie–Weiss temperature. For **4** the Curie constant is $0.167 \text{ emu}\cdot\text{mol}^{-1}\cdot\text{Oe}^{-1}$ and the Curie–Weiss temperature is -0.09 K , showing clearly that **4** is paramagnetic over the entire temperature range. These results and those

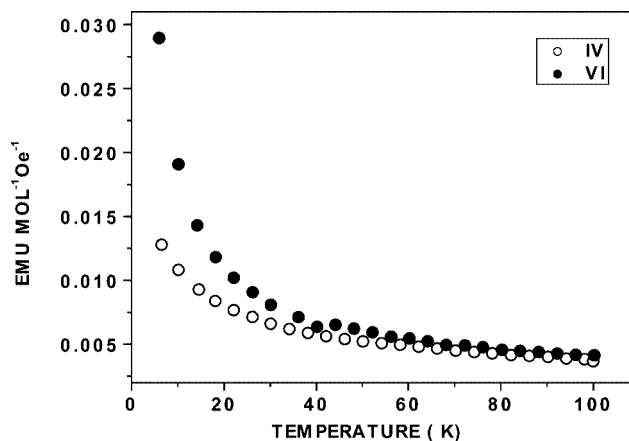


Figure 6. Magnetic susceptibility data for **4** and **6** consistent with paramagnetic behavior above 6 K

of the Mössbauer data provide clear evidence that the spin–lattice relaxation rate in this compound is fast with respect to the characteristic Mössbauer time scale (ca. 100 ns) at all temperatures above 90 K, while spin–spin relaxation can be ruled out in view of the local structure surrounding the iron atoms in next-neighbor molecules. There is no persuasive evidence for iron atom motional anisotropy over the range 90–350 K and the hyperfine parameters are completely reversible in cooling from the upper to the lower temperature of this range. It might be conjectured that the difference in the resonance spectra of compounds such as **4** (as compared to its neutral analogue) and that of ferrocenium ions and ferrocene might be related in some way to the presence of the five methyl groups in the Cp* ring. However, as will be discussed more fully below, resonance spectroscopic data for **8** and its one-electron oxidation product show clearly that the presence of the ring methyl substituents does not play a role in this difference of behavior.

Compound 5

The structure of **5** is very similar to that of **4** except that the second Cp ring is fully methyl substituted in the latter. The Mössbauer parameters, included in Table 1, are very similar to those of **4** and require no further elaboration except as noted below. Since the spectra of **5** again consist of two well-separated resonance maxima over the whole temperature range, the conclusions reached above for **4** relative to the spin–lattice relaxation rate are equally valid in this case.

The temperature dependence of $\ln f$ is shown graphically in Figure 7, from which it is seen that there is a significant change in slope on warming at about 170 K, and a second change in slope (of much smaller magnitude) between 190 and 200 K. To elucidate the origin of these changes a DSC scan was obtained over the temperature range 150–260 K. This scan shows two endotherms, one at about 170 K, the other at 193.5 K. The ΔH and ΔJ values for the latter transition are $1.19 \text{ kJ}\cdot\text{mol}^{-1}$ and $6.16 \text{ J}\cdot\text{mol}^{-1}\cdot\text{K}^{-1}$, respectively, in reasonable agreement with the barriers to internal rotation of the rings in polyene-metal complexes reported in

the literature.^[12] Thus it is inferred that the discontinuity observed in the $\ln f$ data shown in Figure 7 can be associated with the onset of ring rotation/libration of the two Cp* rings relative to the central $\eta^5\text{-P}_5$ ring in the molecular center. As in the case of the structurally closely related **4** there is no significant motional anisotropy of the iron atom observable over the entire temperature range.

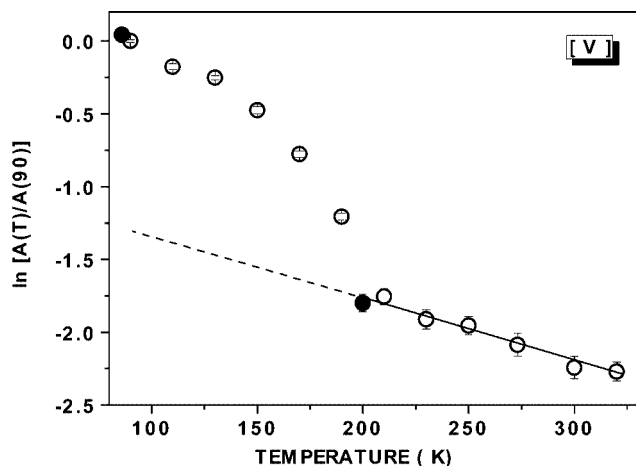


Figure 7. Temperature dependence of $\ln A$ for **5**; the two cooling regime data points (filled circles) were acquired after the 320 K data had been obtained

Compound 6

Finally, the Mössbauer spectra of **6** have been examined in considerable detail, although this molecule does not involve a phospholyl ring atom in its structure. The hyperfine parameters and associated constants are included in Table 1 and are not otherwise remarkable. As noted above, while the two different iron atoms are not resolvable on the basis of their hyperfine interactions, the linewidths (fwhm) in these spectra are again discernably broader than those observed in di-iron compounds in which the two metal atoms are located in identical environments.

The temperature dependence of the IS shows a small amount of curvature at low temperatures, but is reasonably well fitted by a linear regression in the high temperature regime (210–350 K) with a correlation coefficient of 0.997 for 10 data points. The QS is essentially temperature independent, but the area-ratio parameter shows evidence for a significant metal atom motional anisotropy. The temperature dependence of $\ln f$ is linear over the entire temperature range with a correlation coefficient of 0.997 for 19 data points.

As was noted for **4** and **5**, the resonance spectra of **6** consist of well-resolved doublets over the entire range. Since the susceptibility data included in Figure 6 (Curie constant $0.176 \text{ emu}\cdot\text{mol}^{-1}\cdot\text{Oe}^{-1}$ and Weiss constant -10.4 K) again show this compound to be paramagnetic over the entire temperature range, it is concluded that above 86 K, the spin–lattice relaxation rate is again fast compared to the characteristic Mössbauer timescale.

Compound 8 and its One-Electron Oxidation Product

The MS parameters of decamethylferrocene (**8**) are included in Table 1 and have been published previously.^[13] They are included in the present discussion due to the obvious structural relationship of this compound to those of the “double-decker” compounds discussed above. In addition, a detailed MS study of the relaxation spectra of its one-electron oxidation product (as both the BF_4^- and PF_6^- salts) has been carried out, and will be reported separately.^[13] Suffice it to say in the context of the present discussion that the presence of the ring methyl groups plays little role in the rate of the spin–lattice relaxation and the conclusions reached above for this rate in **4**, **5**, and **6** are not related to this ring substitution, but to the presence of two iron atoms in the structure, separated by a η^5 ring moiety which gives rise to the fast relaxation rates observed in these solids.

Systematics of the QS Hyperfine Interaction

The present data set includes structurally very similar compounds with, however, a variable number of ring phosphorus atoms as part of the sandwich architecture. The parameter most influenced by this number is the QS, and the change in the QS as a function of the number of ring phosphorus atoms is summarized graphically in Figure 8 in which the correlation coefficient of the linear regression is 0.994 for eight data points. Clearly, in these structurally closely related compounds the concept of the “partial quadrupole splitting” parameter^[14] appears well justified, with each ring phosphorus atom diminishing the QS by $0.35 \text{ mm}\cdot\text{s}^{-1}$. The relationship summarized in Figure 8 can be accounted for in terms of the molecular orbital treatment of the metal–ligand interactions in ferrocene-like complexes. The fundamental treatment for ferrocene has been well dealt with in the 1965 paper by Collins,^[15] who showed that the Dahl and Ballhausen^[16] treatment (as well as the slightly different scheme of Shustorovich and Dyatkina^[17]) accounts for both the magnitude of the quadrupole interaction in ferrocene, as well as the large reduction in this parameter observed in the one-electron oxidation product. A major contribution to the QS is from the overlap of the e_{2g} and $3d_2$ orbitals, and the decrease in the QS on one-electron oxidation arises from the removal of electron density from the $3d_0$ orbital in the HOMO of the combination. A detailed representation of the MO correlation diagram for the interactions between Fe^{2+} and five-membered cyclic ligands has been given by Frenking.^[18] The corresponding MO-level scheme for P_5 -containing systems has been published by von Schleyer et al.^[19] as applied to a titanium complex. In particular, from the Cp-metal- P_5 MO diagram^[19] it is seen that the HOMO has contributions from metal e_2' , a' , and $e1''$ levels as well as the e_2' π -orbitals of the cyclic P_5 ligand. It is clear from a comparison of these two schemes that the nature of the HOMO in these complexes changes significantly when the $2s2p$ orbitals of carbon are replaced successively by the $3s3p$ orbitals of phosphorus, and it is this change which can account qualitatively for the experimental data summarized in Figure 8.

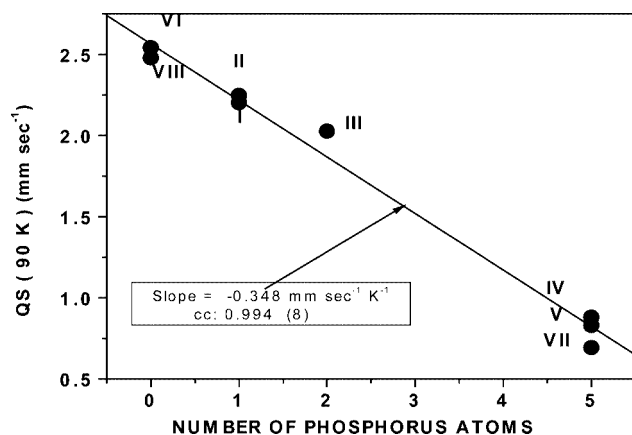


Figure 8. Dependence of the quadrupole hyperfine interaction at 90 K as a function of the number of ring phosphorus atoms in the compounds discussed in the text

Spin Relaxation in Triple-Decker Cations

As noted above, one-electron oxidation of ferrocene, decamethylferrocene (**8**) and related compounds, gives rise to relaxation spectra consisting of an asymmetric broadened resonance envelope, the temperature dependence of which is characteristic of a spin–lattice Raman relaxation process. In contrast, the triple-decker cations examined in the present study (**4**, **5**, and **6**) give rise to well-resolved doublet spectra, albeit with the quadrupole interactions given in Table 1. Since magnetic-susceptibility measurements have shown (in the case of **4** and **6**) that these compounds are paramagnetic at temperatures above 6 K, it is clear that the doublet spectra arise because the spin–lattice relaxation rate is rapid with respect to the characteristic Mössbauer time scale (ca. 10^{-9} s). Thus, at all temperatures of the present study, the resonant (scattering) nucleus sees an average zero hyperfine field, giving rise to narrow resonance lines in the spectra.

X-ray Diffraction Study

The structure of complex **3** was investigated by single-crystal X-ray diffraction. It has the expected sandwich structure (Figure 9). Selected bond lengths and angles are given in Table 2. These values are similar to those for other diphosphaferrocenes.^[20–22] The conformation of the phos-

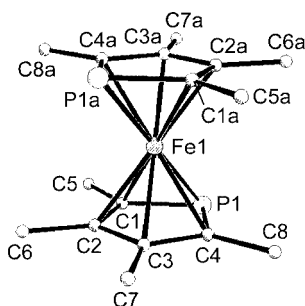


Figure 9. Structure of complex **3** (hydrogen atoms are omitted for clarity)

pholyl rings corresponds to C_{2h} symmetry — the two P atoms are located in opposite directions ($\alpha = 180^\circ$). An analogous conformation was observed for one of two molecules in the unit cell of octaethyldiphosphaferrocene.^[20] Other conformations reported for diphosphaferrocenes include C_{2v} , in which the two phosphorus atoms are eclipsed ($\alpha = 0^\circ$)^[21] and C_1 , in which the P atoms are superposed with the β -carbon of the other ring ($\alpha = 140–145^\circ$).^[22]

Table 2. Selected bond lengths (Å) and angles ($^\circ$) for complex **3**

Fe(1)–P(1)	2.2909(4)	C(1)–P(1)	1.7790(14)
Fe(1)–C(1)	2.0991(13)	C(4)–P(1)	1.7783(15)
Fe(1)–C(2)	2.0674(14)	C(1)–C(2)	1.4241(18)
Fe(1)–C(3)	2.0726(13)	C(2)–C(3)	1.4356(18)
Fe(1)–C(4)	2.0953(14)	C(3)–C(4)	1.422(2)
C(1)–P(1)–C(4)	89.86(7)	C(2)–C(3)–C(4)	111.91(12)
C(2)–C(1)–P(1)	112.61(9)	C(3)–C(4)–P(1)	113.06(10)
C(1)–C(2)–C(3)	112.54(12)		

Cowley et al.^[23] have reported the X-ray structure of the complex $[\text{Ag}\{(\eta\text{-C}_4\text{Me}_4\text{P})_2\text{Fe}\}_2]^+$ in which Ag^+ is coordinated to the lone pairs of phosphorus atoms of **3**. The metal-to-ring distances $\Delta(\text{Fe}\cdots\text{C}_4\text{Me}_4\text{P})$ (1.6851–1.7026 Å, average 1.694 Å) in the $[\text{Ag}\{(\eta\text{-C}_4\text{Me}_4\text{P})_2\text{Fe}\}_2]^+$ cation are longer than the corresponding value in **3** (1.6578 Å). An analogous elongation of Δ in $[\text{Pd}\{(\eta\text{-C}_4\text{Et}_4\text{P})_2\text{Fe}\}_2]^+$ as compared with $[\text{Fe}(\eta\text{-C}_4\text{Et}_4\text{P})_2]$ was also observed.^[20] This elongation is apparently connected with a weakening of direct donation due to a decrease of the donor ability of the ring ligand. Moreover, the phospholyl rings coordinated with the metal atom are in a staggered conformation leading to steric repulsion.

Summary and Conclusions

Eight organometallic compounds of iron, having a variable number of ring-phosphorus-containing ligands, have been examined by temperature-dependent ^{57}Fe Mössbauer spectroscopy, differential-scanning calorimetry, and single-crystal X-ray diffraction. The quadrupole splitting (QS) hyperfine interaction is sensitive to the number of ring P atoms, and decreases as this number increases. The paramagnetic species produced by one-electron oxidation of the neutral precursors show slow spin–lattice relaxation which increases, as expected, with increasing temperature. Compound **3**, the bis-cyclopentadienylphospholyl complex, shows both from Mössbauer recoil-free fraction data and the DSC results that onset of ring rotation gives rise to librational motion affecting the dynamics of the metal atom.

Experimental Section

Complexes **1**,^[24] **2**,^[25] **3**,^[8] **4**,^[26] **5**,^[1] **6**,^[27] **7**^[1] and **8**,^[27] were prepared as described in the literature. All of the compounds examined in this study were rapidly transferred from sealed ampoules to

screw-cap perspex sample holders, sealed with Teflon tape and rapidly cooled to 78 K. Mössbauer spectra were recorded at increasing temperatures (in 20 K steps) to the maximum temperature, and then in a cooling mode to ascertain the reversibility of the data. The details of spectrometer calibration, temperature control and data reduction have been reported previously.^[2] All isomer shifts are reported with respect to the centroid of a room temperature α -Fe absorber spectrum which was also used for spectrometer calibration.

Differential scanning calorimetry data (DSC) were acquired with a Mettler Toledo Star System at warming and cooling rates of 5 K per minute.

Magnetic susceptibility data were acquired in the temperature range 6 to 100 K using a commercial (Quantum Design MPMS-5S) super-conducting interference device (SQUID) magnetometer.

X-ray Crystal Structure Determination: The red plate-like crystals of **3** were grown by slow evaporation of the solvent from a pentane solution. Crystal data: $C_{16}H_{24}FeP_2$ ($M = 334.14$), monoclinic, space group $C2/c$ (no. 15), $a = 14.298(2)$, $b = 12.839(2)$, $c = 8.849(1)$ Å, $\beta = 104.369(3)$, $V = 1573.6(4)$ Å³, $Z = 4$, $d_{\text{calcd.}} = 1.410$ g·cm⁻³, $\mu = 1.146$ mm⁻¹, $F(000) = 704$, crystal size $0.20 \times 0.40 \times 0.60$ mm.

Single-crystal X-ray diffraction experiments were carried out with a Bruker SMART 1000 CCD area detector, using graphite monochromated Mo- K_{α} radiation ($\lambda = 0.71073$ Å, ω -scans with a 0.3° step in ω and 10 s per frame exposure, $2\theta < 60^\circ$) at 120 K. Reflection intensities were integrated using SAINT software,^[28] the absorption correction was applied by semi-empirical method SADABS,^[29] $T_{\text{max}}/T_{\text{min}} = 0.802/0.391$. A total of 6332 reflections were measured, 2075 ($R_{\text{int}} = 0.0179$) independent reflections were used in further calculations and refinement. The structures were solved by direct methods and refined by the full-matrix least-squares method against F^2 in anisotropic (for non-hydrogen atoms) approximation. All hydrogen atoms were located from the difference Fourier syntheses and were included in the final refinement using a rigid motion model in isotropic approximation. The final refinements converged to $R_1 = 0.0377$ [from 1868 unique reflections with $I > 2\sigma(I)$] and $wR_2 = 0.1055$ (from all 2075 unique reflections); the number of refined parameters was 88, GOOF = 0.943, largest diff. peak and hole 1.891 and -0.641 eÅ⁻³. All calculations were performed on an IBM PC/AT using the SHELXTL software.^[30]

CCDC-232591 contains the supplementary crystallographic data for this paper. These data can be obtained free of charge at www.ccdc.cam.ac.uk/conts/retrieving.html [or from the Cambridge Crystallographic Data Centre, 12, Union Road, Cambridge CB2 1EZ, UK; Fax: +44-1223-336033; E-mail: deposit@ccdc.cam.ac.uk].

Acknowledgments

The authors are indebted to Ms. Janet Zoldan of the Technion-Israel Institute of Technology for the careful DSC scans reported herein, Mr. E. Galstyan for the SQUID susceptibility measurements, and Prof. I. Felner for numerous helpful discussions. This research was supported in part by the Israel Academy of Sciences. Z. A. Starikova gratefully acknowledges the financial support of the Russian Foundation for Basic Research (Grant No. 03-03-32214).

- [1] A. R. Kudinov, D. A. Loginov, Z. A. Starikova, P. V. Petrovskii, M. Corsini, P. Zanello, *Eur. J. Inorg. Chem.* **2002**, 3018–3027.
- [2] R. H. Herber, I. Nowik, H. Schottenberger, K. Wurst, N. Schuler, A. G. Müller, *J. Organomet. Chem.* **2003**, 682, 163–171, and references cited therein.
- [3] R. H. Herber, in *Unusual Structures and Physical Properties in Organometallic Chemistry* (Eds.: M. Gielen, R. Willem, B. Wrackmeyer), Wiley, Chichester, **2002**, 207–218.
- [4] R. H. Herber, B. Bildstein, P. Denifl, H. Schottenberger, *Inorg. Chem.* **1997**, 36, 3586–3594, and references cited therein.
- [5] V. M. Rayón, G. Frenking, *Organometallics* **2003**, 22, 3304–3308.
- [6] I. Nowik, R. H. Herber, *Inorg. Chim. Acta* **2000**, 310, 191–195.
- [7] [7a] I. Nowik, R. H. Herber, *J. Phys. Chem. Solids* **2003**, 64, 313–317. [7b] I. Nowik, R. H. Herber, *J. Phys. Chem. Solids* **2003**, 64, 1225.
- [8] F. Nief, F. Mathey, L. Ricard, F. Robert, *Organometallics* **1988**, 7, 921–926; G. de Lauzon, B. Deschamps, J. Fischer, F. Mathey, A. Mitschler, *J. Am. Chem. Soc.* **1980**, 102, 994–1000.
- [9] O. J. Scherer, T. Brück, *Angew. Chem. Int. Ed. Engl.* **1987**, 26, 59, and references cited therein.
- [10] R. H. Herber, O. J. Scherer, *Inorg. Chim. Acta* **2000**, 308, 116–120.
- [11] R. H. Herber, T. P. Hanusa, *Hyperfine Interact.* **1997**, 108, 563–575.
- [12] [12a] C. A. Morrison, S. F. Bone, D. W. H. Rankin, H. E. Robertson, J. A. S. Howell, P. C. Yates, N. Fey, *Organometallics* **2001**, 20, 2309–2320. [12b] P. Comba, T. Gyr, *Eur. J. Inorg. Chem.* **1999**, 1787–1792. [12c] A. Almenningen, A. Haaland, S. Samdal, J. Brunvoll, J. L. Robbins, J. C. Smart, *J. Organomet. Chem.* **1979**, 173, 293–299. [12d] A. Kubo, R. Ikeda, D. Nakamura, *J. Chem. Soc., Faraday Trans. 2* **1986**, 82, 1543–1562. [12e] R. B. Woodward, M. Rosenblum, M. C. Whiting, *J. Am. Chem. Soc.* **1952**, 74, 3458–3459. [12f] M. Rosenblum, R. B. Woodward, *J. Am. Chem. Soc.* **1958**, 80, 5443–5449.
- [13] R. H. Herber, I. Nowik, manuscript to be published.
- [14] G. M. Bancroft, in *Mössbauer Spectroscopy*, J. Wiley & Sons, New York, **1973**, 121–145.
- [15] R. L. Collins, *J. Chem. Phys.* **1965**, 42, 1072–1080.
- [16] J. P. Dahl, C. F. Ballhausen, *Mat. Fys. Medd. Dan. Vid., Selsk.* **1961**, 33; *Chem. Abstr.* **1964**, 61, 1379g.
- [17] E. M. Shustorovich, M. E. Dyatkina, *Dokl. Akad. Nauk* **1959**, 128, 1234–1237; *Chem. Abstr.* **1962**, 57, 1747f; *Chem. Abstr.* **1963**, 58, 7386f, *Chem. Abstr.* **1966**, 64, 18431b.
- [18] G. Frenking, *J. Organomet. Chem.* **2001**, 636, 9–23.
- [19] E. Urnezus, W. W. Brennessel, C. J. Cramer, J. E. Ellis, P. von Ragué Schleyer, *Inorg. Chem.* **2003**, 16, 290–294; see also R. Poli, *ChemTracts* **2003** (16) 290–94.
- [20] X. Sava, L. Ricard, F. Mathey, P. Le Floch, *Organometallics* **2000**, 19, 4899–4903.
- [21] [21a] P. B. Hitchcock, G. A. Lawless, I. Marriano, *J. Organomet. Chem.* **1997**, 527, 305–308. [21b] J. Zakrzewski, A. Klys, M. Bukowska-Strzyzewska, A. Tosik, *Organometallics* **1998**, 17, 5880–5886.
- [22] [22a] G. De Lauzon, B. Deschamps, J. Fescher, F. Mathey, A. Mitschler, *J. Am. Chem. Soc.* **1980**, 102, 994–1000. [22b] S. Qiao, D. A. Hoic, G. C. Fu, *Organometallics* **1998**, 17, 773–774.
- [23] D. A. Atwood, A. H. Cowley, S. M. Dennis, *Inorg. Chem.* **1993**, 32, 1527–1528.
- [24] G. E. Herberich, B. Ganter, *Organometallics* **1997**, 16, 522–524.
- [25] A. R. Kudinov, D. A. Loginov, S. N. Ashikhmin, A. A. Fil'chikov, L. S. Shul'pina, P. V. Petrovskii, *Izv. Akad. Nauk, Ser. Khim.* **2000**, 1647–1649 [*Russ. Chem. Bull.* **2000**, 49, 1637–1639 (Engl. Transl.)].
- [26] O. J. Scherer, T. Brück, G. Wolmershäuser, *Chem. Ber.* **1989**, 122, 2049–2054.
- [27] A. R. Kudinov, M. I. Rybinskaya, Yu. T. Struchkov, A. I.

Yanovskii, P. V. Petrovskii, *J. Organomet. Chem.* **1987**, 336, 187–197.

[28] *SMART v. 5.051 and SAINT v. 5.00, Area detector control and integration software*, **1998**, Bruker AXS Inc., Madison, WI 53719, USA.

[29] G. M. Sheldrick, *SADABS*, **1997**, Bruker AXS Inc., Madison, WI 53719, USA.

[30] G. M. Sheldrick, *SHELXTL-97, v. 5.10*, Bruker AXS Inc., Madison, WI 53719, USA.

Received March 15, 2004

Early View Article

Published Online June 23, 2004